Characteristics of Group III-V Based Multiple Quantum Well Transistor Laser: A simulation based Analysis

Jaspinder Kaur[1], Rikmantra Basu[1]and Ajay Kumar Sharma[2]
[1]Department of Electronics and Communication Engineering, National Institute of Technology Delhi,
[2]Department of Computer Science and Engineering, Dr. B. R. Ambedkar National Institute of Technology Jalandhar, Punjab

Abstract

Simulation based study of InGaAs-GaAs tunnel- injection transistor laser having multiple quantum wells in its base, is presented. We have utilized the luttinger-kohn k.p. model to obtain the various characteristics of multiple quantum well transistor laser including band to band tunneling, free carrier loss, bound state energies, TE gain, TE spontaneous emission rate density etc. Gain and spontaneous emission are calculated by quantum well bound state energies which are obtained through the schrodinger equation. In this paper, simulations are employed to obtain the characteristics of $In_{0.2}Ga_{0.8}As$ having multiple quantum wells in its base.

1. Introduction

Optical transmitters has been the backbone networks for today's user demand applications such as Fiber-to-the-homes (FTTHs), high-speed optical data transmission, and interconnections between computers. In earlier days, laser diodes (LDs) used to meet all these requirement as it has low cost and low power consumption However, due to the damping effect the modulation speed of LDs is limited up to 40 Gb/s. Now a days, transistor laser is a potential candidate for high-speed optical data transmission and replacing LDs [1-4]. The active layer incorporates a Quantum Well (QW) into the base of a Heterojunction Bipolar Transistor (HBT) reported by Nick, Holonyak et al [1, 2]. Under normal active mode of operation, when the excess charge carriers sufficiently injected into the base, population inversion takes place between the CB and VB of the QW. The structure is enclosed in a resonant cavity to provide proper optical feedback leading to self-sustained oscillation [5].

With the incorporation of tunneling phenomenon in a conventional TL structure, switching speed of the device increases as the carriers tunnel from the CB to the VB known as the Band to Band tunneling (BTBT). The main purpose of tunneling is the transfer of carriers through the barrier instead of over the barrier and the tunneling time is much less than the capture and escape time [8].

The analytical and theoretical work of III-V TL has already done by several researchers using laser rate equation and carrier continuity equation. The Feng's group [1-5] has reported extensive experimental work about the characteristics and performance of TL. Same group developed the analytical models for the V-I characteristics, light-output and the optical modulation response. Analytical and numerical models for terminal currents, light -output and optical modulation response of TLs reported by some other groups [7].

The differential gain in the strained QW is estimated by taking into account Fermi golden rule, envelope functions, sub-band energies, polarisation dependent momentum matrix element, 2D density of states and lineshape function [3]. One of the interesting feature is that TL is expected to have a short radiative recombination life-time as compared to the diode lasers (DL) and other conventional optical sources used for telecommunication networks. Another interesting feature is that TL can also give a signal through voltage modulation but diode laser (DL) can give a signal through current modulation [6].

This work demonstrates the simulation of tunnel injection - TL with GaAs alloy as the base material having multiple quantum wells (MQW) structure. Commercially available TCAD simulation tool is used to simulate device structure to study various characteristics such as band to band tunneling, free carrier loss, bound state energies, TE optical gain, TE spontaneous emission rate density etc. Moreover, TE optical gain and spontaneous emission in the active region is achieved with the help of bound state energies that are fully coupled to the electrostatic potential obtained from luttinger-kohn k.p.model. Complete drift-diffusion 2-D carrier transport and laser rate equations are derived by using newton method.

The paper is organized as follows: Section 2 defines the proposed layered structure and simulated band diagram. Section 3 discuss the parameters and models used in the simulation. Section 4 contributes the simulation results and discussion. Section 5 concludes the proposed work

2. 2-D Layered structure

Schematic of two-dimensional (2-D) layered structure of tunnel injection MQW TL is shown in Fig. 1 where $In_{0.2}Ga_{0.8}As$ / GaAs n-p-n heterojunction bipolar transistor structure is used. The InGaP (n-type), GaAs (p-type), and the GaAs (n-type) materials are used for the emitter, base, and collector respectively. The intrinsic $In_{0.2}Ga_{0.8}As$ QWs are inserted in the GaAs base for lasing action. Two separate confinement heterostructure layers of AlAs, generally of 24 nm width act as a wall between MQWs and barriers reducing the leakage current [8]. The collector layer is lattice- matched with the n-type GaAs buffer layer, which helps in the subsequent growth of wells and barriers. The band diagram of the proposed layered device structure is obtained from TCAD simulation tool as shown in Fig. 2. In the present work,

we consider a structure, which is almost identical to the device used in [8]. There are some important modeling implications of the tunnel-injection laser. As, the tunneling occurs directly to low energy bound states, hot carriers are effectively suppressed in the active region and the carrier density can be assumed to be fully 2-D (2-Dimensional). This permits us to avoid the use of capture-escape model to achieve the bound state density in the active region.

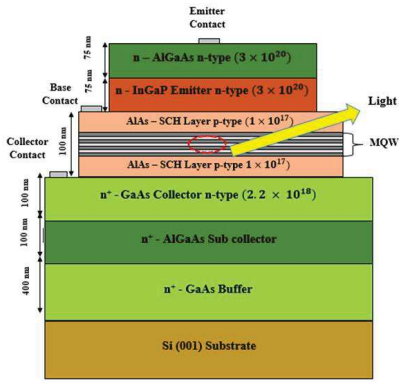

Figure 1. Layered structure of the tunnel –TL (having 3 QWs and 4 barriers in the base layer)

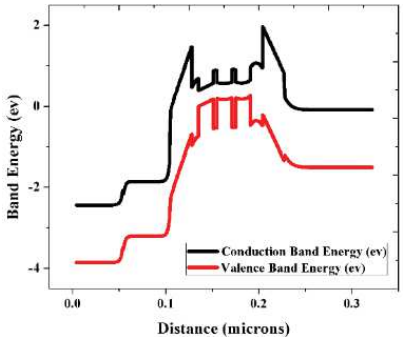

Figure 2. Band diagram of layered structure

Table 1. Parameters of various Device Layers of the Structure

Layer	Composition	Thickness (nm)	Doping (/cm^3)
Emitter	InGaP or AlGaAs	150	n-type 3×10^{20}
SCH Layer	AlAs	24	p-type 1×10^{17}
Barrier	GaAs	4	p-type 4×10^{18}
QW	InGaAs	16	intrinsic
Collector	GaAs	100	n-type 2.2×10^{18}
Sub-collector	AlGaAs	100	n-type 2.2×10^{18}
Virtual Substrate	GaAs	400	-
Substrate	GaAs	400	-

Table 2. Laser Parameters

Laser Parameters	Value
Nmode (Number of modes)	3
Photon energy	0.78
Neff (Effective refractive index)	3.2
Rr (Reflection from the front mirror)	32
Rf (Reflection from the rear mirror)	32
Losses (Losses in the laser)	15
Gainmod (Modal gain for multiband k.p. model)	5
Maxch (Maximum change in photon densities)	2.5

3. Numerical modeling

3.1 Silvaco models and basic laser parameters

All the physical models are established using SILVACO ATLAS/Blaze and laser modules. Here we discuss the details of the laser models specifications and parameters used in simulation.

The drift-diffusion model with Fermi-Dirac statistics is employed. This is a statistical approach to describe the 2D carrier transport. To obtain the optical response in the active region, the deckbuild utilizes the Luttinger-kohn k.p. band structure model. The KP.CV2 parameter is used for the well and barrier region on the models statement. Assume that the quantum wells are coupled. By considering integration over k-space, the optical gain and spontaneous emission are estimated. We use the SPONT model for optical recombination in the well and barrier regions instead of default OPTR. Non local band-to-band tunneling is selected on the model statement by using the BBT.NONLOCAL keyword because the solution will go to relatively high level of tunneling current and set the required direction of tunneling using the QTUNN.DIR parameter on the model statement.

We suppose that the TL is to be worked in the normal transistor operation region without taking into account collector breakdown. Consequently, zener tunnel effect and impact ionization mechanism are not included.

A number of sources for carrier recombination in the QWs have been considered. In the QWs, spontaneous and stimulated emission (radiative recombination) are estimated from the Fermi- Dirac distribution and band structure. We also enable SRH and Auger recombination models. The Auger recombination is given by [6]

$$R_{aug} = \left(C_n n - C_p p\right) \times \left(np - n_i^2\right) \quad (1)$$

where n denotes the electron densities and p represents the hole densities respectively. C_n and C_p indicates the auger coefficients respectively.

The band gap narrowing (BGN) effect are also considered. because it is important in heavily doped regions (greater than 10^{18}/cm^3).

4. Simulation results and discussion

We have obtained different characteristics of our proposed InGaAs MQW TL at 300K by using values of parameters listed in Table 1 [8]. The computed values of various laser parameters for base doping $1 \times 10^{18} cm^{-3}$, for base-emitter voltage ($V_{BE} = 0.4\ to\ 1V$) and collector voltage 2V are given in Table 2. The characteristics of proposed MQW TL structure in this work are mostly obtained through simulation using SILVACO tool.

A. Band to band electron and hole tunneling: Fig. 3(a) and (b) indicates the non-local band to band electron and hole tunneling in the QW regions of the proposed layered structure. From the figure, it is clearly shown that as the base-emitter (V_{BE}) voltage ramped upto 1 V, the band to band electron and hole tunneling rate also increases from 0 to 22.9 cm^{-3}/s and therefore the tunneling current which speed up the device increases as the tunneling rate increases.

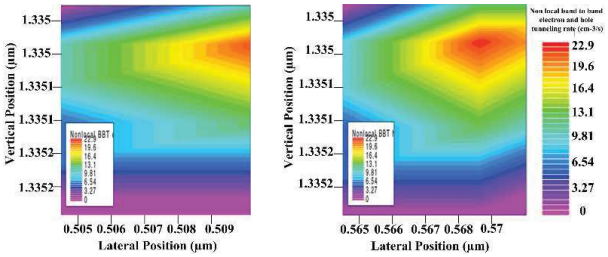

(a) (b)

Fig. 3. Non- local band to band tunneling rate (a) electron tunneling rate (b) hole tunneling rate.

B. Free carrier loss: In actual device structures, different regions are doped with impurities, and consequently, large number of carriers are available in different regions. These free electrons make a transition from a state of wave vector k to another state of wave vector k' in same band by absorbing photons. These free-carrier absorption may be significant because of heavily doped regions and can be explained by Drude-Lorentz equation. From Figure 4 (a), it is observed that the maximum free carrier loss occurs at the emitter region (InGaP) which is very heavily doped ($10^{20}/cm^3$) and Fig. 4 (b) shows its cutline plot.

C. Optical gain: Figure 5 (a) shows the local optical gain along the distance. More and more carrier recombination takes place in the QW regions of the device. Hence maximum optical gain is achieved in the base region and Figure 5 (b) shows its cutline plot.

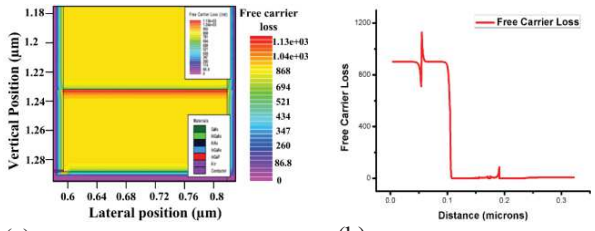

(a) (b)

Fig. 4. (a) Cross sectional view of free carrier loss variation along the distance and (b) its cutline plot.

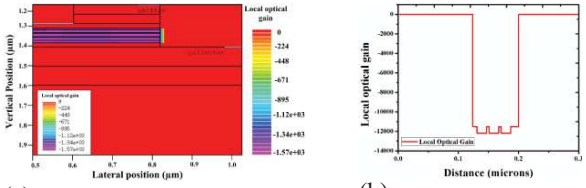

(a) (b)

Fig. 5. (a) Cross-sectional view of local optical gain variation along the distance and (b) its cutline plot.

D. Potential Variation at different voltages:
For a comprehensive physical view of the effect of increasing base-emitter voltage, the electrical potential distribution plot is presented in Fig. 6 (a). As the base to emitter voltage is ramped up to 1V the tunneling phenomenon takes place and the TL is turned on and the ON state current starts to flow and therefore the maximum variation can be seen in the QW regions where the tunneling is occurring and Fig. 6 (b) shows its cutline plot.

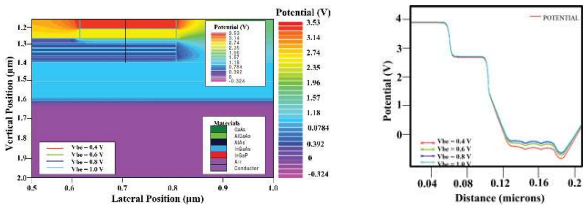

(a) (b)

Fig. 6. (a) Cross sectional view of electrical potential variation and (b) its cutline plot.

E. Effect of band structure below and above threshold:
The band structures are used to find Eigen energies and corresponding wave functions by solving the Schrodinger equation and the optical gain is estimated. Fig. 6 (a) shows the band structure below threshold by consideration of three identical quantum wells but with distinguish electrostatic potential and Fig. 6 (b) shows the 2-3 groups of closely lying bands above threshold, which is contributed by three identical quantum wells and as the electrostatic potential diminishes above threshold these bands merge into each other.

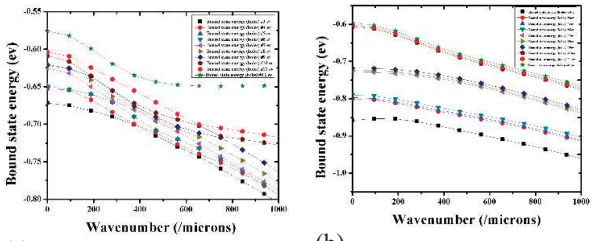

(a) (b)

Fig. 7. (a) band structure below threshold and (b) band structure above threshold

F. TE Gain and spontaneous emission spectra

Figure 8 (a) depicts the TE gain spectra with the variation of photon energy in eV and Figure 8 (b) shows the TE spontaneous emission rate density with the variation of photon energy, respectively. TE and TM optical gain and spontaneous emission spectra is calculated in the active region of tunnel injection - TL using the bound state energies that are fully coupled to the electrostatic potential derived from luttinger- kohn k.p. model. From figure 8 (a), it is seen that the TE gain spectra is obtained above threshold and single mode calculation is performed to obtain the transverse mode of energy about 0.78eV which is very near to the peak of gain spectrum. In Figure 8 (b) spontaneous emission rate is estimated below and above threshold as a function of photon energy. As base-emitter voltage approaches to 0.7 V, spontaneous emission rate is achieved below threshold. On the other hand, when base-emitter voltage goes above 0.7 V, spontaneous emission occurs above threshold.

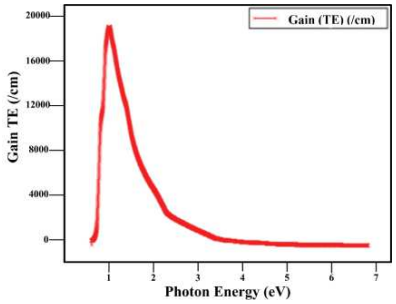

Fig. 8 (b) Variation of TE Gain along the photon energy.

.

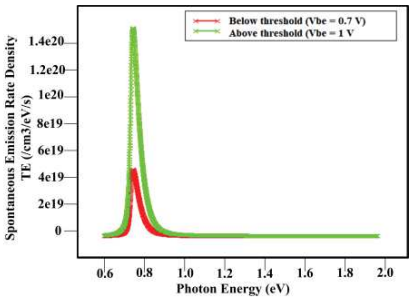

Fig. 8 (b) Variation of TE Spontaneous emission rate density along the photon energy.

5. Conclusion

We have comprehensively simulated the structure of InGaAs based multiple quantum well tunnel injection transistor laser and analyzed with its various characteristics. It is shown that the tunneling rate increases as we increase the base-emitter voltage. Moreover, it is also analyzed that the electrostatic potential diminishes above the threshold and the corresponding TE optical gain and spontaneous emission spectra is obtained. The main motive of this study is to explore group III-V materials in multiple quantum well structure: a motivating and emerging technology.

6. Acknowledgement

Ms. Jaspinder Kaur is thankful to MHRD (India) for providing Junior Research Fellowship (JRF).

7. References

[1] H. W. Then, M. Feng, and N. Holonyak, "The transistor laser: Theory and experiment," *Proc. IEEE*, vol. 101, no. 10, pp. 2271–2298, 2013.

[2] I. Taghavi et al., "Bandwidth enhancement and optical performances of multiple quantum well transistor lasers," *Appl. Phys. Lett.*, vol. 100, no. 23, 2012.

[3] P. K. Basu, B. Mukhopadhyay, and R. Basu, "Analytical model for threshold-base current of a transistor laser with multiple quantum wells in the base," *IET Optoelectron.*, vol. 7, no. 3, pp. 71–76, 2013.

[4] N. Holonyak and M. Feng, "The transistor laser," *IEEE Spectr.*, vol. 43, no. 2, pp. 50–55, 2006.

[5] G. Walter *et al.*, "Laser operation of a heterojunction bipolar light-emitting transistor," vol. 4768, pp. 4–7, 2004.

[6] Z. Duan et al., "Design and epitaxy of 1.5 microm InGaAsP-InP MQW material for a transistor laser.," *Opt. Express*, vol. 18, no. 2, pp. 1501–9, 2010.

[7] R. Basu, B. Mukhopadhyay, and P. K. Basu, "Modeling resonance-free modulation response in transistor lasers with single and multiple quantum wells in the base," *IEEE Photonics J.*, vol. 4, no. 5, pp. 1571–1581, 2012.

[8] N. Kumar et al., "Tunnel injection transistor laser for optical interconnects," *Opt. Quantum Electron.*, vol. 50, no. 3, pp. 1–12, 2018.